31. Special thanks are given to M. Leake for interesting discussions concerning Caloris Basin. We are also grateful to: E. Karkoschka, N. Schneider, and K. Wells for assistance at the telescope and with data analysis; W. Smyth for his help with topics regarding radiation acceleration; K. Linker and D. Yoder for computational assistance; B. Rizk for mapping software; U. Fink for use of his CCD data acquisition system; the UAO telescope allocation committee and scheduling teams for adequate telescope time including the dates required to make these observations. The research was funded by NASA grants NGT 5005065 and NAG2 143 and a Whitaker Foundation grant of the Research Corporation.

5 December 1989; accepted 26 June 1990

Hole Density Dependence of the Critical Temperature and Coupling Constant in the Cuprate Superconductors

M.-H. WHANGBO AND C. C. TORARDI

A bond valence sum (BVS) analysis was performed for the p-type cuprate superconductors. The superconducting critical temperature T_c versus in-plane Cu-O BVS correlation for copper is grouped into classes and subclasses. Only within a class or subclass for which the nonelectronic effect is constant does the variation of the in-plane Cu-O BVS reflect the corresponding change in the hole density n_H of the CuO_2 layers. This study strongly suggests that the T_c for every class or subclass of the superconductors is an inverted parabolic function of n_H, and so is the coupling constant λ for Cooper pair formation.

IN UNDERSTANDING THE SUPERCONductivity of the cuprate superconductors it is vital to know what structural or electronic factors govern the magnitudes of their superconducting critical temperatures T_c. The T_c values of the p-type cuprate superconductors have been correlated with a number of parameters, which include the hole densities (n_H) per CuO_2 unit in the CuO_2 layers (*1–9*), the Madelung potentials (*10, 11*), the electronegativities (*12–15*), the in-plane Cu-O bond lengths (*16, 17*), the electronic densities of states at the Fermi level (*18*), the bond valence sums (BVSs) (*19–23*), and the hole density to effective mass ratios (*24*). Oxidation of the CuO_2 layers (that is, hole doping) removes electrons from the x^2-y^2 bands which have antibonding character in the in-plane Cu-O bonds (*25, 26*). As n_H increases, therefore, the in-plane Cu-O bond length (r_{Cu-O}) is shortened. In addition to this electronic factor, the in-plane r_{Cu-O} is also controlled by the nonelectronic factor (*16, 17*) (for example, steric strain) associated with the cations located at the 9-coordinate sites adjacent to the CuO_2 layers (see Fig. 1, top). With the increasing size of the 9-coordinate site cations, the in-plane Cu-O bond is lengthened to reduce the extent of the resulting steric strain. The T_c versus in-plane r_{Cu-O} plot of the p-type cuprate superconductors is grouped into three classes distinguished by the size of the 9-coordinate site cations (that is, La-, Sr-, and Ba-classes) (*16, 17*) because of the combined electronic and nonelectronic effects. The Sr- and Ba-classes contain subclasses which are further distinguished by a secondary nonelectronic factor associated with the number of CuO_2 layers per unit cell or the cation substitution in the rock salt layers. Every class or subclass of the T_c versus in-plane r_{Cu-O} plot shows a maximum, so that every class or subclass of the p-type cuprate superconductors possesses an optimum hole density (n_{opt}) for which the T_c is maximum ($T_{c,max}$) (*16, 17*).

By definition, the bond valence of an in-plane Cu-O bond should increase with the shortening of its length (*27, 28*). Since the in-plane r_{Cu-O} decreases with increasing n_H, the BVS of an in-plane Cu atom obtained only from its in-plane Cu-O bonds (hereafter referred to as the in-plane BVS) is expected to increase with increasing n_H. Therefore, a T_c versus in-plane BVS plot should have a maximum as in the corresponding T_c versus in-plane r_{Cu-O} plot. The steric factor associated with the 9-coordination site cation affects the in-plane r_{Cu-O} value and hence the corresponding in-plane BVS value. Therefore, the T_c versus in-plane BVS plot for the p-type cuprate superconductors should separate into La-, Sr-, and Ba-classes and their subclasses as in the case of the T_c versus in-plane r_{Cu-O} plot. This expectation is borne out as will be shown below. The present work strongly suggests that the T_c for each class or subclass is an inverted parabolic function of the in-plane BVS or the hole density n_H. This relationship leads to an important constraint that the coupling constant λ for Cooper pair formation is an inverted parabolic function of n_H.

The bond valence s_i of a bond i is defined

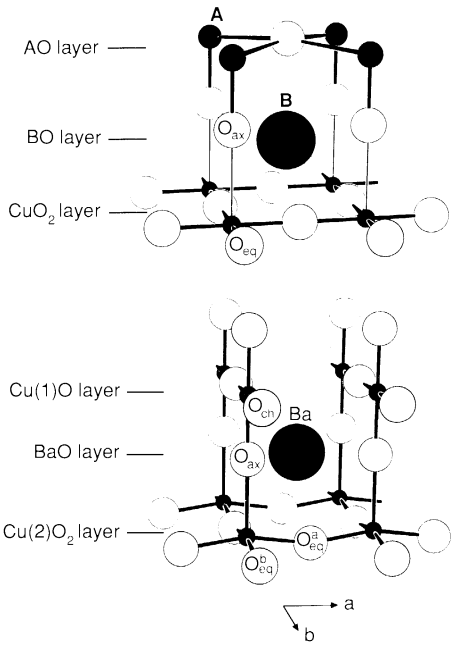

Fig. 1. (**Top**) Schematic diagram (*42*) showing the arrangement of atoms around a 9-coordinate site in p-type cuprate superconductors. The cations are represented by shaded circles, and the oxygen atoms by unshaded circles. The 9-coordinate cation B is La^{3+}, Sr^{2+}, and Ba^{2+} in the La-, Sr-, and Ba-class superconductors, respectively. (**Bottom**) Schematic diagram (*42*) showing the arrangement of atoms around the Ba^{2+} cation in $YBa_2Cu_3O_y$ ($y = 7$), where the cations are indicated by shading.

Table 1. Calculated α, V_{opt}, and RMSE (root-mean-square error) values from the least-squares fitting of the La-, Sr- and Ba-classes and their subclasses with the equation* $\Delta T_c = -\alpha(\Delta V)^2$.

Compounds	$\alpha \times 10^{-4}$	V_{opt}	RMSE†
Ba-class	2.72 ± 0.18	2.05	7.1
Sr-class	3.20 ± 0.53	2.15	11.0
La-class[a]	2.46 ± 0.53	2.27	4.9
$(Tl_{2-x}Cd_x)Ba_2CuO_6$ subclass[b]	6.09 ± 1.01	2.04	7.7
$Bi_2Sr_2(Ca_{1-x}Y_x)Cu_2O_8$ subclass[c]	5.78 ± 0.70	2.12	4.8
$(Tl_{0.5}Bi_{0.5})Sr_2(Ca_{1-x}Y_x)Cu_2O_7$ subclass[d]	4.85 ± 1.04	2.18	10.0

*BVS calculated using the in-plane r_{Cu-O} values from: [a]Tarascon *et al.* (*30*) for $La_{2-x}Sr_xCuO_4$; [b]Parise *et al.* (*41*); [c]Groen and de Leeuw (*32*); [d]Huang *et al.* (*33*). †Standard deviations of the observed T_c values from the quadratic fits.

M.-H. Whangbo, Department of Chemistry, North Carolina State University, Raleigh, NC 27695–8204.
C. C. Torardi, Central Research and Development Department, E. I. du Pont de Nemours and Company, Experimental Station, Wilmington, DE 19880–0356.

Table 2. Calculated β, n_{opt}, and RMSE (root-mean-square error) values from the least-squares fitting of the La-class and the $Bi_2Sr_2(Ca_{1-x}Y_x)Cu_2O_8$ subclass with the equation* $\Delta T_c = -\beta(\Delta n_H)^2$.

Compounds	Hole density used	$\beta \times 10^{-3}$	n_{opt}	RMSE†
La-class[a]	n_H	1.92 ± 0.14	0.181	2.7
	n_H (BVS)	1.92 ± 0.41	0.180	4.8
$Bi_2Sr_2(Ca_{1-x}Y_x)Cu_2O_8$ subclass[b]	n_H	4.19 ± 0.48	0.187	7.7
	n_H(BVS)	4.19 ± 0.51	0.188	4.7

*T_c and n_H values are from: [a]Torrance *et al.* (*2*) for $La_{2-x}Sr_xCuO_4$; [b]Groen *et al.* (*4*). †Standard deviations of the observed T_c values from the quadratic fit.

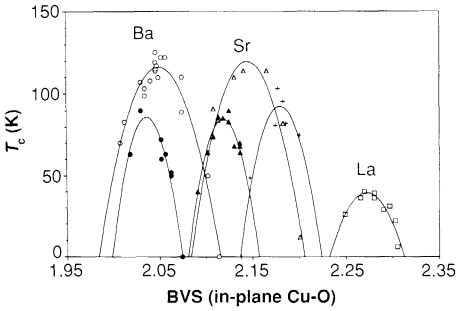

Fig. 2. T_c versus in-plane BVS plot for the La-, Sr-, and Ba-class and subclass superconductors. The symbols are defined as: ○, Ba-class; △, Sr-class; □, La-class; ●, $(Tl_{2-x}Cd_x)Ba_2CuO_6$ subclass; ▲, $Bi_2Sr_2(Ca_{1-x}Y_x)Cu_2O_8$ subclass; +, $(Tl_{0.5}Bi_{0.5})Sr_2(Ca_{1-x}Y_x)Cu_2O_7$ subclass. The solid line passing through each class or subclass represents the quadratic function of in-plane BVS obtained by least-squares fitting.

as $s_i = \exp[(r_o - r_i)/0.37]$, where r_i is the length of the bond i, and r_o is the constant that depends upon the atoms constituting the bond (*28*). For a metal atom surrounded by several identical ligands with bond lengths r_i, its BVS is given by the sum of all the bond valences $\sum s_i$. The bond valence s_i may be viewed as the amount of electrons the metal atom loses to form the bond i. Thus, the BVS of the metal atom is a measure of the total amount of electrons it loses, that is, the formal oxidation state of the atom. The lengths of the chemical bonds in crystalline materials are determined by the electronic factor, which reflects the amounts of electrons in the bonds, and also by the nonelectronic factor (for example, steric strain), which alters the bond lengths without changing the amounts of electrons in the bonds. BVS values are strongly affected by the steric factor: for example, the BVS values of the formal Sn^{4+} ions in the K_2NiF_4-phase A_2SnO_4 (A = Sr, Ba) are calculated to be 4.88 and 3.92 for A = Sr and Ba, respectively (*29*). As the A-cation (that is, Sr^{2+} and Ba^{2+}) size increases, the Sn-O bond length increases thereby decreasing the BVS value of the Sn^{4+}-cation. Thus, BVS values cannot be used as a measure of formal oxidation states unless the steric factor is constant.

Due to the in-plane nature of the x^2-y^2 band orbitals (*25, 26*), a change in n_H directly affects the in-plane Cu-O bond lengths. Consequently, only the in-plane BVS values can be a meaningful measure for the n_H values. Figure 2 shows how the T_c values of the p-type cuprate superconductors are related to their in-plane BVS values for copper, which we calculate with r_o = 1.679 Å for the Cu-O bonds (*28*). For the BVS analysis, relatively accurate Cu-O bond lengths are needed. In obtaining the T_c versus in-plane BVS plot of Fig. 2, we employ all the data points of the Ba-class from our T_c versus in-plane r_{Cu-O} plot (*16*) and the data points of the La-class (that is, $La_{2-x}Sr_xCuO_4$) by Tarascon *et al.* (*30*). Because the CuO_2 layers of the Sr-class typically exhibit modulation and buckling (*31*), we use only the data points of the Sr-class derived from single crystal or powder structure refinement studies (*16, 17, 32, 33*). Figure 2 clearly demonstrates that the T_c versus in-plane BVS for copper is grouped into La-, Sr-, and Ba-classes, and that the Sr- and Ba-classes each contain subclasses, just as in the case of the T_c versus in-plane r_{Cu-O} correlation (*16, 17*). As shown by a solid line passing through each class or subclass, the T_c values are well approximated by a quadratic function of in-plane BVSs (see below), and each class or subclass shows a maximum. With the larger 9-coordination site cation, the in-plane Cu-O bond is more stretched out so that the maximum of the corresponding T_c versus in-plane BVS plot is shifted toward the direction of smaller BVS values. Due to this steric effect of the 9-coordinate site cation, the absolute in-plane BVS values cannot reflect the effective valences of the in-plane Cu atoms. Within each class or subclass, however, the steric effect of the 9-coordinate site cation is fairly constant so that a change in the in-plane BVS value reflects the effect of the electronic factor and therefore is a reliable measure of the change in n_H. It is noted that the inverted parabolic shape of the Sr and Ba classes may simply be an envelope associated with a series of inverted parabolas from their respective subclasses. As expected, the T_c versus out-of-plane BVS plot (not shown) does not exhibit any direct correlation that can be explained in terms of changes in n_H.

The atomic arrangement around the Ba^{2+} cation in $YBa_2Cu_3O_y$ (y = 7) is schematically shown in Fig. 1, bottom. The oxygen atoms of the Cu-O chains (that is, O_{ch}) are gradually lost as y decreases from 7 to 6 (*34*), so that the coordination number of Ba changes from 10 to 8. For $y > 6.4$ the Cu-O chain runs along the b-axis direction and thus the in-plane (that is, equatorial) Cu-O bonds along the **a** and **b** directions [Cu(2)-$O_{eq,a}$ and Cu(2)-$O_{eq,b}$, respectively] are not equivalent. As a function of y, the overall change of the out-of-plane (that is, axial) Cu-O bonds is much larger than that of the in-plane Cu-O bonds (*19*). The hole density in the CuO_2 layers of $YBa_2Cu_3O_y$ is greater for $y > 6.4$ than for $y < 6.4$ (*5–9*). Thus, according to the electronic factor (that is, hole doping in the CuO_2 layers) alone, a bond shortening is expected for both Cu(2)-$O_{eq,a}$ and Cu(2)-$O_{eq,b}$ as y increases from 6 to 7. The Cu(2)-$O_{eq,a}$ bond length follows this prediction, but the Cu(2)-$O_{eq,b}$ bond does not (*19*). The latter is explained by the steric effect of the O_{ch} atoms, because the formation of the Cu(1)-O_{ch} chains stretches out the b-axis length thereby lengthening the Cu(2)-$O_{eq,b}$ bond. Such a steric effect is absent along the a-axis direction. Figure 3A

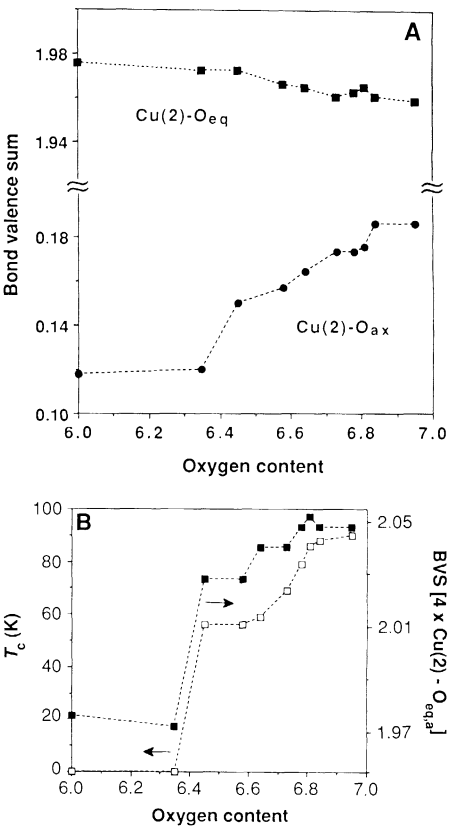

Fig. 3. (**A**) BVS values calculated for the in-plane and out-of-plane Cu-O bonds of $YBa_2Cu_3O_y$ as a function of y. (**B**) Plots of BVS [4 × Cu(2)-$O_{eq,a}$] versus y (■) and T_c versus y (□) for $YBa_2Cu_3O_y$.

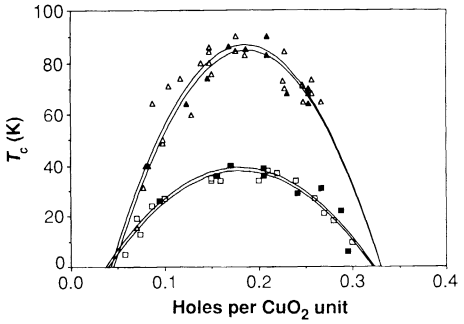

Fig. 4. Comparison of the T_c versus n_H correlations (△, □) with the T_c versus n_H (BVS) correlations (▲, ■). The symbols are defined as: △, ▲, $Bi_2Sr_2(Ca_{1-x}Y_x)Cu_2O_8$ subclass; □, ■, La-class. The solid line passing through each class or subclass represents the quadratic equation of n_H or the calculated n_H (BVS) obtained by least-squares fitting.

shows the BVS values calculated for the Cu(2)-O_{ax} and four Cu(2)-O_{eq} bonds {that is, 4 × Cu(2)-O_{eq} for $y < 6.4$ and [2 × Cu(2)-$O_{eq,a}$] + [2 × Cu(2)-$O_{eq,b}$] for $y > 6.4$}. As anticipated from the bond length trends, the BVS change as a function of y is much stronger for the out-of-plane Cu-O bonds than for the in-plane Cu-O bonds. The BVS for the in-plane Cu-O bonds does not increase but decreases as y varies from 6 to 7, because the Cu(2)-$O_{eq,b}$ bond lengthening (caused by the steric strain of the O_{ch} atoms) has a greater effect on the BVS than does the Cu(2)-$O_{eq,a}$ bond shortening (induced by the hole doping). Thus, only the Cu(2)-$O_{eq,a}$ bond length change can be related to the n_H change in the CuO_2 layers, since the Cu(2)-$O_{eq,a}$ bonds are not affected by the steric effect of the O_{ch} atoms. In the absence of the O_{ch} atom steric effect, the Cu(2)-$O_{eq,b}$ bond length would vary as the Cu(2)-$O_{eq,a}$ bond does. Thus, the BVS values calculated for 4 × Cu(2)-$O_{eq,a}$ would be a reasonable measure for the n_H values. Figure 3B shows the BVS [4 × Cu(2)-$O_{eq,a}$] versus y plot, which exhibits step-like increases in the BVS values as a function of y and thereby implying that the n_H values would also have step-like increases as y varies from 6 to 7. These step-like patterns are quite similar to those found for the T_c versus y plot, also shown in Fig. 3B. Thus, as suggested by Cava *et al.* (*19*), the plateaus of the T_c versus y plot for $YBa_2Cu_3O_y$ (y = 6 to 7) appear to reflect step-like increases in n_H as y varies from 6 to 7.

It is clear from our discussions above that only the in-plane Cu-O bond lengths can be correlated with the CuO_2 layer hole density, but both the electronic and nonelectronic factors affect the in-plane Cu-O bond lengths and thus their bond valences. In discussing hole density changes in the CuO_2 layers on the basis of the in-plane Cu-O bond lengths or their bond valences, it is important to realize that, only within a closely related class or subclass for which the nonelectronic effect is constant, the in-plane Cu-O bond lengths or their bond valences are a reliable measure of the n_H values of the CuO_2 layers.

To simplify the notational problem in the remainder of our work, the in-plane BVS term will be denoted by V, and the optimum in-plane BVS corresponding to the $T_{c,\,max}$ value by V_{opt}. It is convenient to introduce the following quantities: $\Delta T_c = T_c - T_{c,max}$ and $\Delta V = V - V_{opt}$. Then, the T_c and V values of each class or subclass can be correlated with the expression

$$\Delta T_c = -\alpha(\Delta V)^2 \qquad (1)$$

where α is a positive constant. Table 1 summarizes the α and V_{opt} values determined for the classes and subclasses of Fig. 2 by least-squares fitting with Eq. 1, which provides a good correlation between the T_c and V values for all the classes and subclasses of the p-type cuprate superconductors. Within a class or subclass, it is highly probable that the change ΔV is proportional to the corresponding change in hole density, that is, $\Delta n_H \propto \Delta V$, where $\Delta n_H = n_H - n_{opt}$. Therefore, the T_c and n_H values for each class or subclass should be governed by the expression

$$\Delta T_c = -\beta(\Delta n_H)^2 \qquad (2)$$

where β is a positive constant. We test how well Eq. 2 describes the available experimental T_c and n_H values by considering the La-class (*2*) and the $Bi_2Sr_2(Ca_{1-x}Y_x)Cu_2O_8$ (*4*) subclass. Results of our least-squares fitting with Eq. 2 for these two systems are summarized in Fig. 4 and Table 2. Clearly, Eq. 2 provides a good correlation between the T_c and n_H values. For the La-class and the $Bi_2Sr_2(Ca_{1-x}Y_x)Cu_2O_8$ subclass, Eqs. 1 and 2 provide equally good correlations, from which one obtains the following relationship

$$n_H = (\alpha/\beta)^{1/2}\Delta V + n_{opt} \qquad (3)$$

To probe the accuracy of this relationship between Δn_H and ΔV, we calculate the n_H values of the La-class and the $Bi_2Sr_2(Ca_{1-x}Y_x)Cu_2O_8$ subclass from the observed in-plane Cu-O bond lengths by using Eq. 3 on the basis of the α and ΔV values (from the T_c versus in-plane BVS plot) as well as the β and n_{opt} values (from the T_c versus n_H plot). These calculated n_H values may now be referred to as n_H(BVS). Figure 4 shows both the T_c versus n_H and the T_c versus n_H(BVS) plots for the two systems. As can be seen from Fig. 4 and Table 2, the T_c versus n_H(BVS) plots are in essence identical with the corresponding experimentally determined T_c versus n_H plots. Thus, Eq. 3 provides an excellent correlation between Δn_H and ΔV. Since Eq. 1 is good for all known p-type cuprate superconductors, it is expected from Eqs. 1 and 3 that Eq. 2 is valid for all known p-type cuprate superconductors, unless lattice instability sets in at a certain value of n_H thereby giving rise to a structural phase transition as in the case of $La_{2-x}Ba_xCuO_4$ (*35*).

With the constant $\eta = \beta/T_{c,max}$, Eq. 1 can be written as $T_c = T_{c,max}[1-\eta(\Delta n_H)^2]$, which becomes equivalent to Eq. 4

$$T_c = T_{c,max} \exp\,[-\eta(\Delta n_H)^2] \qquad (4)$$

under the condition that $|\Delta n_H| << (1/\eta)^{1/2}$. According to the β values (Table 2) and the $T_{c,max}$ values of the La-class and the $Bi_2Sr_2(Ca_{1-x}Y_x)Cu_2O_8$ subclass, the constant η is about 50. Therefore, Eq. 4 is valid for $|\Delta n_H| << 0.14$, which is readily satisfied for most n_H values around n_{opt}. For pairing due to exchange of phonons, spin-fluctuations, or combined charge fluctuations and lattice distortions, the T_c and the coupling constant λ are governed by the expression (*36–39*)

$$T_c \simeq \omega \exp\,[-(1+\lambda)/(\lambda-\delta)] \qquad (5)$$

where ω is the average energy of the fluctuations of the pairing field and δ is a small correction term. In the Bardeen-Cooper-Schrieffer (BCS) theory (*36, 37*), ω corresponds to the Debye temperature, λ is the electron-phonon coupling constant, and δ is the effective Coulomb pseudopotential of the order of 0.1. Relevance of Eq. 5 for the cuprate superconductors has been suggested (*38, 39*). It is noted that Eq. 4 is formally equivalent to Eq. 5. If the small correction term δ of Eq. 5 is neglected, Eqs. 4 and 5 lead to the following expression for λ

$$\lambda = [(\zeta - 1) + \eta\,(\Delta n_H)^2]^{-1} \qquad (6)$$

where $\zeta = \ln(\omega/T_{c,max})$. In all the p-type cuprate superconductors, $T_{c,max} \lesssim 125$ K, so that $\zeta > 2$ when $\omega \simeq 1000$ K. Therefore, $(\zeta - 1) >> \eta\,(\Delta n_H)^2$, so that Eq. 6 can be further simplified as $\lambda \simeq B - A\,(\Delta n_H)^2$, where A and B are positive constants given by $A = \eta/(\zeta-1)^2$ and $B = 1/(\zeta-1)$. Since $\Delta n_H = n_H - n_{opt}$, the coupling constant λ is finally expressed as

$$\lambda = \lambda_H + \lambda_0 \qquad (7)$$

where

$$\begin{aligned} \lambda_H &= A\,n_H\,(2\,n_{opt} - n_H) \\ \lambda_0 &= B - A\,n_{opt}^2 \end{aligned} \qquad (8)$$

λ_0 is independent of n_H, so that the n_H-dependence of λ is then contained in the λ_H term. Essentially, the n_H-dependence of λ_H is given by $\lambda_H \propto n_H\,(C\text{-}n_H)$, where C is a

positive constant. Thus, the magnitude of λ_H is governed by two opposing factors: One factor increases λ_H linearly with increasing n_H (that is, $\lambda_H \propto n_H$) while the other factor decreases λ_H linearly with increasing n_H (that is, $\lambda_H \propto C\text{-}n_H$). It is important to note that the λ_H versus n_H plot has the shape of an inverted parabola (with the maximum at $n_H = C/2$). This character of λ_H is ultimately responsible for the inverted parabolic shape observed for the T_c versus n_H plots. It is crucial to understand the exact origin of the $\lambda_H \propto n_H$ ($C\text{-}n_H$) relationship. As plausible reasons, we suggest the following: Cooper pair formation is enhanced with shortening the average distance between holes and thus with increasing n_H, which might lead to the $\lambda_H \propto n_H$ relation. Certain physical parameters associated with the in-plane Cu-O bond (for example, the in-plane Cu-O bond polarizability and the softness of the in-plane Cu-O bond stretching or bending vibration) decrease their magnitudes with increasing n_H. If such physical parameters are responsible for Cooper pair formation, the $\lambda_H \propto C\text{-}n_H$ relation might result. Then, combination of the two opposing effects would lead to the relationship $\lambda_H \propto n_H(C\text{-}n_H)$, which is a necessary condition that any satisfactory pairing mechanism must accommodate. Note that λ consists of an n_H-dependent term, λ_H, and an n_H-independent term, λ_0. It is possible that λ_0 originates from the electron-phonon coupling mechanism and λ_H from a new pairing mechanism yet to be determined.

REFERENCES AND NOTES

1. M. W. Shafer, T. Penney, B. L. Olsen, *Phys. Rev. B* **36**, 4047 (1987).
2. J. B. Torrance, *et al.*, *Phys. Rev. Lett.* **61**, 1127 (1988).
3. W. A. Groen, D. M. de Leeuw, L. F. Feiner, *Physica C* **165**, 55 (1990).
4. W. A. Groen, D. M. de Leeuw, G. P. J. Geelen, *ibid.*, p. 305.
5. T. Penney, M. W. Shafer, B. L. Olsen, *ibid.* **162–164**, 63 (1989).
6. M. W. Shafer, T. Penney, B. L. Olsen, R. L. Greene, R. H. Koch, *Phys. Rev. B* **39**, 2914 (1989).
7. D. B. Mitzi *et al.*, *ibid.* **38**, 6667 (1988).
8. R. Liang, M. Itoh, T. Nakamura, *Physica C* **157**, 83 (1989).
9. Y. Tokura, J. B. Torrance, T. C. Huang, A. I. Nazzal, *Phys. Rev. B* **38**, 7156 (1988).
10. Y. Ohta, T. Tohyama, S. Maekawa, *Physica C* **166**, 385 (1990).
11. J. B. Torrance and R. M. Metzger, *Phys. Rev. Lett.* **63**, 1515 (1989).
12. R. Asokamani and R. Manjula, *Phys. Rev. B* **39**, 4217 (1989).
13. S. Balasubramanian and K. J. Rao, *Solid State Commun.* **71**, 979 (1989).
14. J. Gopalakrishnan, M. A. Subramanian, A. W. Sleight, *J. Solid State Chem.* **80**, 156 (1989).
15. D. A. Nepela and J. M. McKay, *Physica C* **158**, 65 (1989).
16. M.-H. Whangbo *et al.*, *ibid.*, p. 371.
17. C. C. Torardi, D. Jung, D. B. Kang, J. Ren, M.-H. Whangbo, *Mat. Res. Soc. Symp. Proc.* **156**, 295 (1989).
18. R. S. Markiewicz and B. G. Giessen, *Physica C* **160**, 497 (1989).
19. R. J. Cava, *et al.*, *ibid.* **165**, 419 (1990).
20. I. D. Brown, *J. Solid State Chem.* **82**, 122 (1989), and references therein.
21. J. L. Tallon and G. V. M. Williams, paper (A-V.3) presented at the meeting of the European Materials Research Society, Strasbourg, France, 29 May to 1 June 1990.
22. D. M. de Leeuw, W. A. Groen, L. F. Feiner, E. E. Havinga, *Physica C* **166**, 133 (1990).
23. J. B. Parise and E. M. McCarron, paper presented at the Materials Research Society Symposium, Boston, 27 November to 2 December 1989.
24. Y. J. Uemura *et al.*, *Phys. Rev. Lett.* **62**, 2317 (1989).
25. M.-H. Whangbo, M. Evain, M. A. Beno, J. M. Williams, *Inorg. Chem.* **26**, 1829 (1987).
26. M.-H. Whangbo, M. Evain, M. A. Beno, J. M. Williams, in *High-Temperature Superconducting Materials: Synthesis, Properties and Processing*, W. E. Hatfield and J. H. Miller, Jr., Eds. (Dekker, New York, 1988), p. 181.
27. I. D. Brown and R. D. Shannon, *Acta Crystallogr. A* **29**, 266 (1973).
28. I. D. Brown and D. Altermatt, *Acta Crystallogr. B* **41**, 244 (1985).
29. Calculated on the basis of the crystal structures reported by Weiss and Faivre (*40*). The r_0 value of the Sn-O bond is 1.905 Å (*28*).
30. J. M. Tarascon, L. H. Greene, W. R. McKinnon, G. W. Hull, T. H. Geballe, *Science* **235**, 1373 (1987).
31. Y. Le Page, W. R. McKinnon, J.-M. Tarascon, P. Barboux, *Phys. Rev. B* **40**, 6810 (1989), and references therein.
32. W. A. Groen and D. M. de Leeuw, *Physica C* **159**, 417 (1989).
33. Y. T. Huang, R. S. Liu, W. N. Wang, P. T. Wu, *Jpn. J. Appl. Phys.* **28**, L1514 (1989).
34. J. D. Jorgensen *et al.*, *Phys. Rev. B* **36**, 3608 (1987).
35. J. D. Axe *et al.*, *Phys. Rev. Lett.* **62**, 2751 (1989); A. R. Moodenbaugh, Y. Xu, M. Suenaga, T. J. Fokerts, R. N. Shelton, *Phys. Rev. B* **38**, 4596 (1988).
36. J. Bardeen, L. N. Cooper, J. R. Schrieffer, *Phys. Rev.* **108**, 1175 (1957).
37. W. L. McMillan, *ibid.* **167**, 331 (1968).
38. K. H. Bennemann, *Solid State Commun.* **67**, 431 (1988).
39. J. Ruvalds, *Phys. Rev. B* **35**, 8869 (1987).
40. R. Weiss and R. Faivre, *Comptes Rendus. Heb. Seanc. Acad. Sci.* **248**, 106 (1959).
41. J. B. Parise, N. Herron, M. K. Crawford, P. L. Gai, *Physica C* **159**, 255 (1989).
42. Structural figures were drawn with the assistance of the ORTEP program, written by C. K. Johnson, 1976.

43. We thank J. Cameron and J. J. Novoa for their help in the error analysis. Work at North Carolina State University is supported by the Office of Basic Energy Sciences, Division of Materials Sciences, U.S. Department of Energy under grant DE-FG05-86ER45259.

25 June 1990; accepted 25 July 1990

Thin Films of *n*-Si/Poly-$(CH_3)_3$Si-Cyclooctatetraene: Conducting-Polymer Solar Cells and Layered Structures

MICHAEL J. SAILOR, ERIC J. GINSBURG, CHRISTOPHER B. GORMAN, AMIT KUMAR, ROBERT H. GRUBBS,* NATHAN S. LEWIS*

The optical and electronic properties of thin films of the solution-processible polymer poly-$(CH_3)_3$Si-cyclooctatetraene are presented. This conjugated polymer is based on a polyacetylene backbone with $(CH_3)_3$Si side groups. Thin transparent films have been cast onto *n*-doped silicon (*n*-Si) substrates and doped with iodine to form surface-barrier solar cells. The devices produce photovoltages that are at the theoretical limit and that are much greater than can be obtained from *n*-Si contacts with conventional metals. Two methods for forming layered polymeric materials, one involving the spin-coating of preformed polymers and the other comprising the sequential polymerization of different monomers, are also described. An organic polymer analog of a metal/insulator/metal capacitor has been constructed with the latter method.

ELECTRONICALLY CONDUCTIVE POLYMERS are currently of interest for their possible applications in electronics (*1*), nonlinear optics (*2*), and solar energy conversion systems (*3*). To date, most synthetic routes to these polymers have produced insoluble, intractable materials with fibrillar or porous morphologies. Consequently, the conventional synthetic routes to conducting organic polymers have precluded the fabrication of uniform, well-defined electronic or optical structures. Recently, ring-opening metathesis polymerization (ROMP) has allowed the preparation of soluble, processible, conductive polyacetylenes (*4, 5*). In this work we demonstrate that this new synthetic route can be exploited to fabricate thin films of conducting organic polymers for possible use in several electronic and optical applications. These include semiconductor/organic polymer junctions for solar cells and layered polymeric structures for potential use as polymer-based capacitors or optical waveguides.

Our synthetic procedure utilized the tungsten carbene complex $W(CHC(CH_3)_3)(N\text{-}2,6\text{-}(CH(CH_3)_2)_2\text{-}C_6H_3)(OC(CH_3)(CF_3)_2)_2$ (*6*) to catalyze the ROMP route with substituted cyclooctatetraenes (COT),

Arnold and Mabel Beckman Laboratory of Chemical Synthesis and the Arthur A. Noyes Laboratory of Chemical Physics, The Division of Chemistry and Chemical Engineering, California Institute of Technology, Pasadena, CA 91125.

*To whom correspondence should be addressed.